

Design of Carbon-Carbon Ylides

Muhammad Yasir Mehboob^a, Emran Masoumifeshani^a, Zahra Badri^a, Cina Foroutan-Nejad^{a*}

a. Institute of Organic Chemistry, Polish Academy of Sciences, Kasprzaka 44/52, 01-224, Warsaw,
Poland.

Corresponding Author's Email: cina.foroutan-nejad@icho.edu.pl

Abstract

Here, we have reported the computational design of a new class of ylides, elusive carbon-carbon ylides featuring zwitterionic σ -bonds, derived from the norbornane-2,6-dione framework. Utilizing the state-of-the-art computational methods, we have demonstrated that appropriate substitutions on this scaffold can stabilize a carbanion at **C1** and a carbocation at **C7** without orbital overlap, ensuring a zwitterionic electronic structure akin to a CC-ylide. Large singlet-triplet energy gaps guarantee that these species do not adopt a diradical ground state. Time-dependent DFT computations further have revealed small T1-S1 energy gaps, suggesting potential applications of similar scaffolds in thermally activated delayed fluorescence (TADF) materials. Our analyses have identified the cation on **C7** as the most reactive site on the molecule towards unwanted reactions, leading to the degradation of the ylides. With their unique electronic structure, CC-ylides present new opportunities for unexplored chemical reactivity and functional material design.

Introduction

A carbon-carbon double bond, comprising a σ -bond and a π -bond, can break into an adjacent triplet diradical when one of the two sp^2 -hybridized alkylene groups twists by 90° relative to the other, disrupting the overlap between their atomic p-orbitals. This triplet diradical state is often the first electronically excited state of alkenes, except when the neighboring alkylene groups are sterically restricted from planarization and radical centers are stabilized through significant delocalization in the ground state. Recent advances in stereo-electronic tuning of hydrocarbons have enabled the stabilization of such diradicals as the ground state of the molecules.^[1,2] Another notable excited state of alkenes is the high-energy zwitterionic singlet state. In this state, one neighboring carbon's p-orbital is fully occupied while the p-orbital of the other remains unoccupied.^[3,4] This state corresponds to a carbon-carbon ylide (CC-ylide). To the best of our knowledge, no stable ground-state molecule corresponding to this zwitterionic CC-ylide form has been synthesized or computationally predicted. This is despite substantial interest in zwitterionic species, diradicals, and zwitterionic diradicals within both theoretical and experimental chemistry.^[1,5–17]

To create a CC-ylide with a zwitterionic σ -bond, the overlap between neighboring atomic p-orbitals must first be disrupted to prevent the formation of a conventional π -bond. Additionally, the near-degeneracy of the two p-orbitals should be eliminated by stabilizing the carbanion and carbocation through stereoelectronic engineering of structure. Substitution of the carbanion and carbocation centers via electron-withdrawing and -donating groups, respectively, is the first step to stabilize the ionic centers. Further stabilization of the carbanion can be achieved by enforcing a pyramidal geometry. Small bicyclic frameworks, such as bicyclo[2.2.1]heptane, bicyclo[2.1.1]hexane, and bicyclo[1.1.1]pentane, meet all the structural requirements for this purpose. The rigidity of these frameworks prevents **C1**, the branching carbon, to adopt a planar

geometry. This rigidity allows for the localization of a carbanion with sp^3 hybridization at **C1** when electron-withdrawing groups are substituted at **C2/C6** and **C3/C5** in the norbornane framework or their corresponding carbons in other frameworks, **Figure 1a**. On the other hand, a carbocation at the one-carbon bridge, i.e., **C7** in norbornane framework, can planarize and be stabilized by introducing an electron-donating substituent. Using state-of-the-art computational tools, we propose the norbornane-2,6-dione framework, **Figure 1b**, as a basis for CC-ylides, featuring adjacent carbocation and carbanion centers that form a zwitterionic carbon-carbon σ -bond. This molecular structure is envisioned as a target for future synthesis. In the following sections, we detail our approach to stabilizing the ion pair, demonstrate the spatial localization of the adjacent ions, evaluate the stability of these species in condensed phases, and explore potential applications.

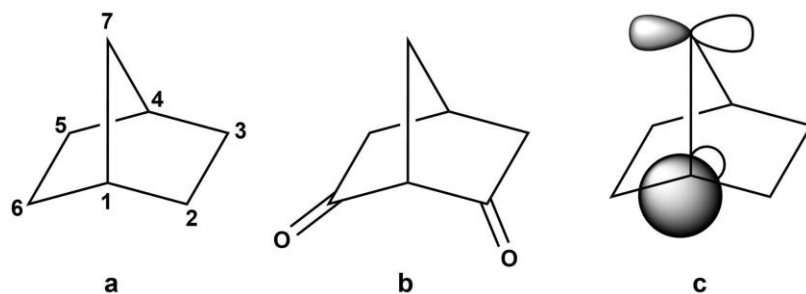
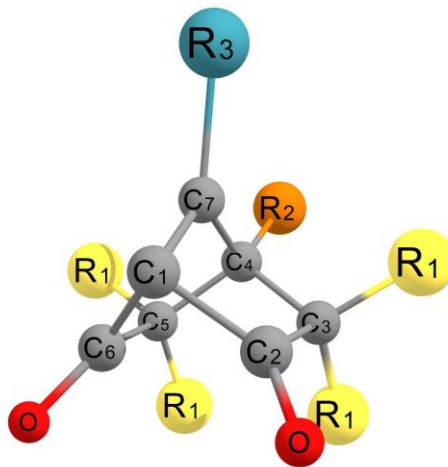


Figure 1. (a) The IUPAC numbering system for the norbornane framework, (b) the structure of norbornane-2,6-dione, and (c) a schematic representation of the empty p orbital on **C7** and the sp^3 hybrid orbital on **C1** in the norbornane framework.

Results and discussion

Recent studies on anti-Bredt olefins suggest that a two-membered carbon bridge in bicyclo[2.2.1]heptane, or longer bridges in larger bicyclic species, can sustain a double bond.^[18–22] However, our CASPT2 computational analysis indicates that a double bond cannot form between the branching carbon (**C1**) and the one-member carbon bridge (**C7**) in bicyclo[2.2.1]heptane, see **Figure 1a** for numbering. The ground state of a hypothetical

bicyclo[2.2.1]hept-4(7)-ene, or as conventionally known, 7-norbornene, is a triplet diradical that is 16 kcal·mol⁻¹ lower in energy than the singlet state corresponding to the double-bond. See **Figure 1c** for a simplified representation of two orthogonal orbitals, a p-orbital on the sp²-hybridized **C7** and a sp³-hybridized orbital on **C1**, accommodating the electrons of triplet diradical state of bicyclo[2.2.1]hept-4(7)-ene. Substitution however can stabilize a zwitterionic singlet state versus a diradical triplet.



- | | |
|--|--|
| 1: (R ₁ :CN, R ₂ :CN, R ₃ :DMAP) | 8: (R ₁ :F, R ₂ :F, R ₃ :DMA) |
| 2: (R ₁ :CN, R ₂ :CN, R ₃ :DMA) | 9: (R ₁ :F, R ₂ :F, R ₃ :OMe) |
| 3: (R ₁ :CN, R ₂ :CN, R ₃ :OMe) | 10: (R ₁ :F, R ₂ :F, R ₃ :OPh) |
| 4: (R ₁ :CN, R ₂ :CN, R ₃ :OPh) | 11: (R ₁ :F, R ₂ :H, R ₃ :OPh) |
| 5: (R ₁ :CN, R ₂ :H, R ₃ :DMAP) | 12: (R ₁ :H, R ₂ :H, R ₃ :DMA) |
| 6: (R ₁ :CN, R ₂ :H, R ₃ :OPh) | 13: (R ₁ :H, R ₂ :H, R ₃ :OMe) |
| 7: (R ₁ :F, R ₂ :F, R ₃ :DMAP) | 14: (R ₁ :H, R ₂ :H, R ₃ :OPh) |

Figure 2. Schematic representations of the structures of 14 molecules derived from the norbornane-2,6-dione framework with S-T energy gaps greater than 10 kcal·mol⁻¹. R₁ and R₂ represent hydrogen (H) or electron-withdrawing groups such as fluoro (F) and cyano (CN). R₃ is an electron-donating group that stabilizes the cation on C7. In this study, we examined 4-dimethylaminophenyl (DMAP), methoxy (OMe), phenoxy (OPh), and dimethylamine (DMA) as electron-donating groups.

Figure 2 depicts 14 molecules derived from substituted norbornane-2,6-dione, each with a singlet-triplet energy gap of at least 9 kcal·mol⁻¹ (one-third of an eV) and zwitterionic carbon-

carbon σ -bond character, i.e., CC-ylide. To confirm that the singlet states correspond to zwitterionic structures, we employ tools from molecular orbital theory and quantum chemical topology. **Table 2** provides data on atomic charges, singlet-triplet energy gaps, and NBO^[23] analyses, including the hybridization and occupancy of the lone pair on **C1** for molecules **1** to **14**.

Table 1. The singlet-triplet Gibbs free energy gap (corrected for zero-point vibrational energies) in kcal.mol⁻¹, atomic charges, and NBO derived hybridization and occupancy of the lone-pair electrons on **C1** in molecules **1** to **14**; all data are computed in the gas-phase.

Molecules	S-T gap	$q^{\text{NBO}}_{\text{C}1}$	$q^{\text{NBO}}_{\text{C}7}$	Hbrid _{LP}	Occ _{LP}	$q^{\text{QTAIM}}_{\text{C}1}$	$q^{\text{QTAIM}}_{\text{C}7}$	$q^{\text{Mulliken}}_{\text{C}1}$	$q^{\text{Mulliken}}_{\text{C}7}$
1	41.5	-0.58	0.35	2s 22.24%, 2p 77.24%	1.63	-0.12	-0.03	-0.28	-0.26
2	59.6	-0.59	0.54	2s 23.73%, 2p 75.74%	1.65	-0.10	0.69	-0.29	-0.21
3	14.8	-0.57	0.76	2s 25.85%, 2p 73.50%	1.65	-0.07	0.84	-0.16	0.08
4	15.3	-0.61	0.76	2s 26.85%, 2p 72.51%	1.67	-0.09	0.81	-0.19	-0.04
5	10.4	-0.58	0.34	2s 21.73%, 2p 77.75 %	1.62	-0.13	-0.03	-0.24	-0.14
6	13.7	-0.58	0.74	2s 26.47%, 2p 72.89%	1.65	-0.08	0.78	-0.15	0.04
7	9.6	-0.54	0.28	2s 26.03%, 2p 73.44%	1.64	-0.20	-0.04	-0.10	-0.24
8	32.5	-0.56	0.42	2s 26.79%, 2p 72.69%	1.66	-0.18	0.63	-0.15	-0.13
9	22.0	-0.61	0.61	2s 29.88%, 2p 69.55%	1.69	-0.18	0.74	-0.18	0.05
10	15.1	-0.52	0.59	2s 27.49%, 2p 71.85%	1.61	-0.13	0.70	-0.03	-0.05
11	15.2	-0.60	0.67	2s 29.86%, 2p 69.52%	1.70	-0.17	0.71	-0.15	0.10
12	25.1	-0.63	0.51	2s 28.88%, 2p 70.67%	1.73	-0.21	0.60	-0.15	-0.05
13	16.3	-0.66	0.67	2s 31.34%, 2p 68.16%	1.75	-0.22	0.69	-0.19	0.13
14	10.4	-0.64	0.67	2s 30.55%, 2p 68.92%	1.72	-0.19	0.66	-0.15	0.12

Atomic charges are not uniquely definable; therefore, we analyze trends and agreements among three different atomic charge models. Atomic charges derived from natural bond orbital (NBO) theory consistently indicate that **C1** accommodates a negative charge, with NBO analysis confirming a lone pair occupancy between 1.62 and 1.75 electrons. Molecules with more electron-withdrawing groups at positions **C3**, **C4**, and **C5** tend to exhibit a lower s-character in the lone pair orbitals and relatively lower occupancy. Despite some variations, the carbanion's

hybridization can be consistently assigned as sp^3 , with an average s-orbital contribution of 26.98% across all species. On the other hand, the positive charge on **C7** decreases significantly when substituted with 4-dimethylaminophenyl (DMAP) or dimethylamine (DMA), which are expected to delocalize the positive charge, compared to methoxy (OMe) and phenoxy (OPh) substituents with an electronegative oxygen.

The charges of topological atoms, defined within the context of quantum theory of atoms in molecules (QTAIM), follow similar trends as NBO charges with two main differences. QTAIM suggests that **C7** carries a slight negative charge when substituted with DMAP. Furthermore, the QTAIM charges on **C1** are notably smaller in magnitude than the corresponding NBO charges but remain consistently negative. Although Mulliken charges are among the least reliable due to their dependency on the basis set sizes, they still align with the trends observed in NBO and QTAIM charges. Mulliken charges also indicate a slight negative charge on **C7** in all species substituted with DMAP and DMA.

The morphology of the canonical and natural molecular orbitals supports the trends observed in the atomic charges. The dihedral angle between the lone-pair orbital on **C1** and the π^* orbitals of the carbonyl substitutions at positions 2 and 6 prevents efficient overlap and stabilization via resonance. This is consistent with the carbonyl bond lengths, which are all approximately 1.2 Å, corresponding to carbon-oxygen double bonds. The natural HOMOs clearly display a lone pair localized in an sp^3 -type orbital. Interestingly, the canonical HOMOs are similar to those obtained from NBO localization, also corresponding to the lone pair mainly localized on **C1**. The LUMOs represent π^* orbitals that are consistent with the carbocation on **C7**, **Figure 2**. Notably, the LUMO becomes more localized on the carbon atom when **C7** is substituted with an alkoxy substituent, due to the presence of electronegative oxygen. It is important to note that

positive charge on **C7** is stabilized by resonance through π -donation in all species. The bond lengths of **C7-C(DMAP)**, **C7-N(DMA)**, **C7-O(OMe)**, and **C7-O(OPh)** are all slightly shorter than normal single bonds, **Table S1**. Other chemical bond indicators also conform to a partial π -character, *vide infra*.

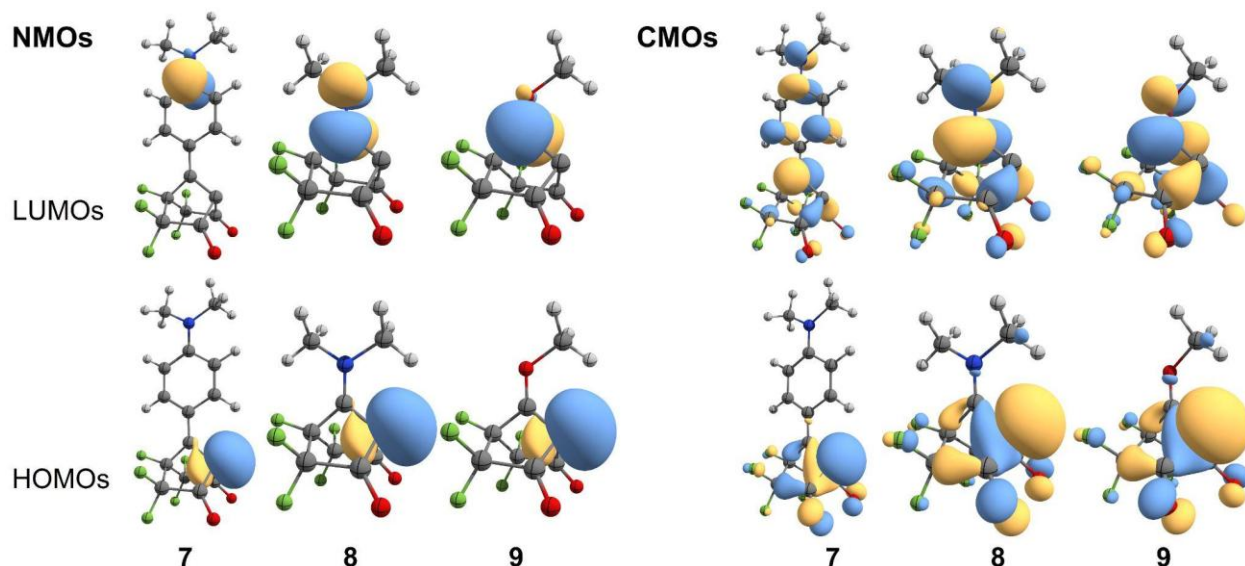


Figure 3. Natural and canonical frontier molecular orbitals of molecules **7**, **8**, and **9**, featuring three different donor groups on **C7**; DMAP, DMA, and OMe, respectively.

Due to the presence of strong electron-withdrawing groups on the majority of our model systems and low occupancy of the lone-pairs on **C1**, NBO analysis shows a relatively high non-Lewis population. In order to verify legitimacy of the MO-based analyses, we also employed the theory of interacting quantum atoms (IQA)^[24–27] within the framework of quantum theory of atoms in molecules (QTAIM)^[28] and QTAIM’s topological analysis to obtain a thorough picture of the bonding in our model systems. Analyzing the map of the Lapacian of electron density reveals all electron concentration and depletion regions in a molecule. Electron concentration between atoms is often associated with electron sharing and covalency, but local electron concentration on atoms represent lone-pairs. Our analysis reveals a localized concentration of electron density on **C1**,

evidenced by a (3, -3) critical point in the Laplacian of electron density across all species, as shown in **Figure 4**. Examination of the local properties of the (3, -3) critical points on **C1** in compounds **1** to **14** reveals consistently high local electron density values, ranging narrowly from 0.261 to 0.279 au. Furthermore, the significantly negative values of both the Laplacian of electron density and the energy density indicate strongly localized electron density, consistent with the presence of a lone pair of electrons, as presented in **Table 2**.

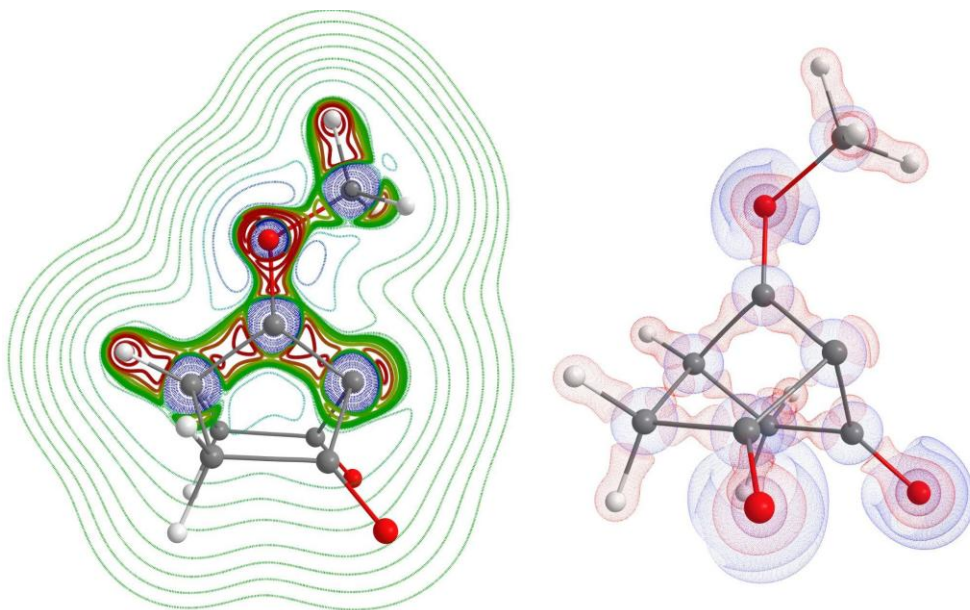


Figure 4. Contour map (left) and three-dimensional isosurface (right) of the Laplacian of electron density for compound **13**. Blue and red regions indicate electron depletion and concentration, respectively. The green color on the contour map corresponds to values close to zero. In both representations, an electron concentration region is evident on **C1**, corresponding to a lone pair of electrons. The three-dimensional isosurface map illustrates regions with values of -0.5 (red) and 0.5 (blue) atomic units.

The **C1–C7** bond lengths range from 1.420 to 1.495 Å, which is shorter than the typical C–C single bond length, **Table 3**. This observation aligns with the delocalization index (DI) values between these carbons, which measure the number of shared electrons and correlate with bond order. The DI provides insight into the stabilization mechanism of the cation on **C7**, too. As noted

earlier, **C7** forms relatively short bonds with the attached electron-donating groups. The DI between **C7** and its neighboring carbon in DMAP ranges from 1.36 in molecule **7** to 1.46 in molecule **1**, indicating π -donation and formation of partial π -bonds. For molecules **2**, **8**, and **12**, where the neighboring atom is nitrogen, the DI decreases to 1.27–1.36 due to nitrogen's higher electronegativity compared to carbon. Finally, in molecules with OMe or OPh substituents on **C7**, the DI between **C7** and the electronegative oxygen drops further, ranging from 1.02 in molecule **14** to 1.13 in molecule **3**, **Table S1**.

Table 2. Properties of the (3, -3) critical point, in the Laplacian of electron density near **C1**, corresponding to a lone pair. Electron density, $\rho(r)$, Laplacian of electron density, $L(r)$, and energy density, $H(r)$, are presented in atomic units

Molecule	$\rho(r)$	$L(r)$	$H(r)$	Molecule	$\rho(r)$	$L(r)$	$H(r)$
1	0.270	-0.864	-0.464	8	0.265	-0.837	-0.453
2	0.273	-0.887	-0.472	9	0.271	-0.879	-0.467
3	0.275	-0.900	-0.477	10	0.261	-0.803	-0.444
4	0.278	-0.929	-0.485	11	0.277	-0.925	-0.482
5	0.271	-0.876	-0.467	12	0.276	-0.928	-0.479
6	0.275	-0.906	-0.477	13	0.279	-0.948	-0.486
7	0.263	-0.830	-0.450	14	0.279	-0.944	-0.486

Within the framework of IQA theory, the interatomic interaction energy between two atoms can be decomposed into ionic, $V_{\text{Ion}}(m, n)$, and covalent, $V_{\text{Cov}}(m, n)$, components. The ionic component, also known as the Coulombic component of the interaction energy, is typically positive for purely covalent bonds. This indicates unfavorable electrostatic interactions between two uncharged atoms. For reference, the ionic energy component for the C–C bonds in ethane, ethene, and ethyne is 15.7, 43.4, and 84.1 $\text{kcal}\cdot\text{mol}^{-1}$, respectively, at the same computational level.^[29] The ionic contribution to the **C1–C7** bond in our models is positive, despite the charge

differences between the atoms, except in systems **12** and **13**, **Table 3**. This is due to the unfavorable interaction between the atomic dipole moments of the QTAIM atoms.

Table 3. Delocalization indices (DI) between selected carbon atoms, bond lengths (\AA) interatomic interaction energy ($V_{\text{Int}}(1, 7)$), ionic contribution ($V_{\text{Ion}}(1, 7)$), and covalent component of the interaction energy ($V_{\text{Cov}}(1, 7)$) for the **C1–C7** bond, as well as the covalent component of interaction energy between **C2/C6** and **C7**, and **C3/C5** and **C7** ($\text{kcal}\cdot\text{mol}^{-1}$). All values are computed at M06-2X/def2-TZVP computational level.

Molecules	DI(1, 7)	BL(1, 7)	$V_{\text{Int}}(1, 7)$	$V_{\text{Ion}}(1, 7)$	$V_{\text{Cov}}(1, 7)$	DI(2, 7)	DI(3, 7)	$V_{\text{Cov}}(2, 7)$	$V_{\text{Cov}}(3, 7)$
1	1.02	1.478	-189.4	9.2	-198.6	0.08	0.06	-9.6	-7.2
2	0.98	1.474	-183.0	11.0	-193.9	0.08	0.06	-10.2	-7.5
3	1.02	1.447	-186.2	16.6	-202.8	0.10	0.06	-12.2	-7.8
4	1.04	1.442	-192.9	13.3	-206.1	0.10	0.06	-12.8	-7.8
5	1.03	1.495	-190.5	9.3	-199.8	0.08	0.08	-10.1	-10.2
6	1.04	1.445	-189.8	15.2	-205.0	0.10	0.07	-11.9	-8.4
7	1.08	1.460	-199.5	9.3	-208.8	0.09	0.06	-9.9	-7.4
8	1.02	1.465	-197.7	2.4	-200.1	0.08	0.06	-9.9	-7.4
9	1.09	1.430	-212.0	3.8	-215.8	0.10	0.07	-12.3	-8.0
10	1.14	1.420	-212.0	10.7	-222.7	0.09	0.06	-11.0	-7.1
11	1.10	1.431	-210.6	5.6	-216.2	0.11	0.07	-12.7	-8.3
12	1.02	1.467	-199.3	-0.9	-198.5	0.10	0.08	-12.0	-9.0
13	1.10	1.430	-215.9	-0.1	-215.8	0.12	0.09	-15.4	-10.0
14	1.13	1.423	-217.3	3.3	-220.5	0.10	0.07	-12.7	-8.1

On the other hand, the covalent component of the interaction energy, corresponding to the exchange-correlation contribution, is purely stabilizing, ranging from -193.9 to -222.7 $\text{kcal}\cdot\text{mol}^{-1}$,

Table 3. These values are larger than that of a typical single bond. For comparison, the covalent energy components of the interaction energy between carbon atoms in ethane, ethene, and ethyne are -189.6, -330.4, and -481.4 $\text{kcal}\cdot\text{mol}^{-1}$, respectively.

The carbonyl groups at positions 2 and 6 of the molecules serve a dual role. In addition to stabilizing the carbanion on **C1** through induction, they engage in electron exchange with **C7** which results in the delocalization of the positive charge by electron sharing between these carbons. This is evident from the delocalization indices between **C2/C6** and **C7** compared to those between **C3/C5** and **C7**, as shown in **Table 3**. The accompanying covalent component of the interaction energy, $V_{\text{Cov}}(n, m)$, correlates with the delocalization indices as expected from the relationship between these two terms as described elsewhere.^[30–32]

Our bonding analyses consistently reveal a unique electron arrangement around **C1** and **C7** in the studied model systems, supporting the notion of a CC-ylide. It is crucial to highlight that, regardless of the employed bonding analyses, the formal charges of these species in a classical Lewis structure align with those expected for ylides. The singlet electronic state of these systems is significantly lower in energy than the triplet diradical. Without the possibility of double-bond formation between the two three-coordinated carbon atoms, the two electrons can either remain weakly coupled as a singlet diradical or localize as a formal lone pair on a single carbon atom. However, the large singlet-triplet gaps observed in these systems are inconsistent with a singlet diradical. Consequently, even in the absence of detailed bonding analyses, the sole possible description of these species is as CC-ylides with a zwitterionic bond.

To investigate the nature of the excited states in our carbon ylides, we conducted time-dependent DFT computations using the Tamm-Dancoff approximation (TDA).^[33] A notable trend observed across all model systems is that in gas phase the first singlet excited state (S_1) is only a few meV higher in energy than the triplet state (T_1), **Table 4**. This suggests the potential for thermally activated delayed fluorescence (TADF),^[34–36] in some of the studied species and even the possibility of singlet-triplet inversion^[37] through targeted structural modifications. Vertical

singlet to triplet energy gap of the molecules is within the range of approximately 1.0 to 2.5 eV. Interestingly, both the S₁ and T₁ states originate from a HOMO (lone pair) → LUMO (π^*) transition. The S₁-T₁ energy gap decreases in species with more electron-withdrawing groups on positions **C3**, **C4**, and **C5**. In the polar solvent DMF, the energy gap between the ground state and the excited states increases significantly, as DMF stabilizes the zwitterionic ground state. Moreover, the second excited triplet state (T₂) becomes lower in energy than S₁. For the excited states energies in DMF see **Table S2** in the **Supporting Information**.

Table 4. Energies of the first (T₁) and second (S₁) excited states for molecules **1** to **14** in eV. All transitions correspond to HOMO → LUMO excitations. In every case, the first excited state is a triplet (T₁), while the second excited state is a singlet (S₁).

Molecule	T ₁ Energy	S ₁ Energy	Molecule	T ₁ Energy	S ₁ Energy
1	1.27	1.32	8	2.42	2.52
2	2.49	2.57	9	1.95	2.06
3	1.60	1.68	10	1.51	1.90
4	1.71	1.81	11	1.69	1.85
5	1.22	1.27	12	2.34	2.42
6	1.60	1.72	13	1.93	2.06
7	1.06	1.14	14	1.65	1.93

A major challenge in the chemical synthesis of species such as carbon ylides is their stability in condensed phases. Molecules containing both a cation and an anion are highly reactive, making them prone to rapid degradation through reactions with other active species or their precursors. To assess the stability of carbon ylides, we conducted a case study on molecule **13**, evaluating two potential reactions that could lead to its degradation. Molecule **13** was specifically chosen for two reasons: (1) it lacks electron-withdrawing groups apart from the carbonyls,

rendering the carbanion center highly reactive, and (2) its substitution at **C7** with a small methoxy group offers only minimal steric and electronic protection to the cationic center, making it an excellent candidate for evaluating the maximum reactivity of CC-ylides

The first potential reaction for degradation of ylides is their reaction with their precursors. For the precursor, we modeled a system in which both **C1** and **C7** are hydrogenated, leaving the carbonyl carbons as the sole reactive sites, susceptible to nucleophilic attack by the carbanionic center (**C1**). This reaction can produce four distinct products, depending on the regiochemistry, with their relative energies falling within a narrow range of $1.1 \text{ kcal}\cdot\text{mol}^{-1}$. The computed transition state energy for this reaction in DMF is $21.7 \text{ kcal}\cdot\text{mol}^{-1}$ for the formation of the most stable product. This relatively high activation energy suggests that the reaction between molecule **13** and the carbonyl group in the precursor or similar species will proceed slowly enough to allow formation of molecule **13**.

CC-ylides can dimerize through bond formation between **C1** and **C7** of two separate molecules. Our computations indicate that the singlet dimer, with a separated pair of cation and anion, is $26.8 \text{ kcal}\cdot\text{mol}^{-1}$ more stable than the isolated monomers. DFT calculations suggest that also a triplet dimer lies just $1.1 \text{ kcal}\cdot\text{mol}^{-1}$ below the singlet state. The dissociation energy of the dimer is only 33% of the C-C bond dissociation energy in ethane, highlighting significant repulsion between the two fragments. It is plausible that dimerization energy decreases further when bulkier substituents are present on C7. In the case of molecule **13**, we did not identify a transition state corresponding to dimerization via coupling between the **C1** carbanion and **C7** carbocation. This was further confirmed by a relaxed scan of the **C–C** bond distance in the dimer, which exhibited only one potential energy well as expected of the coupling of an ion pair. Therefore, to achieve a

stable CC-ylide, the presence of bulky groups on C7 is crucial to introduce steric hindrance and prevent dimerization.

Conclusions

In this study, we introduce a new class of ylides; carbon-carbon ylides (CC-ylides) featuring a zwitterionic σ -bond, based on the norbornane-2,6-dione framework. Our extensive first-principles computations demonstrate that proper substitution within this scaffold enables the stabilization of a carbanion at **C1**, the branching carbon, and a carbocation at **C7**, the one-carbon bridge. The intrinsic rigidity of the norbornane-2,6-dione structure prevents significant orbital overlap between the charged centers, preserving their zwitterionic nature of the CC-ylides.

Our extensive computational analyses indicate that large singlet-triplet energy gaps preclude a diradical ground state, further supporting the classification of these species as CC-ylides. Detailed bonding analyses, utilizing NBO, IQA, and QTAIM methodologies, consistently reinforce this description. Besides, time-dependent DFT using TDA approximation computations reveal small T1-S1 energy gaps, suggesting that these molecules may serve as promising candidates for thermally activated delayed fluorescence (TADF) materials.

Finally, to achieve stable CC-ylides, steric protection of the carbocation at **C7** is essential, as this position is the most susceptible to unwanted reactions. Our results highlight the potential of CC-ylides as a new family of molecules with applications in novel synthesis, materials science, and particularly in the design of functional organic materials.

Methods

In this work, we examined 44 structures across three frameworks — bicyclo[2.2.1]heptane, bicyclo[2.1.1]hexane, and bicyclo[1.1.1]pentane. Various electron-donating groups were tested at **C7**, including t-butyl, 4-methylphenyl, 4-methoxyphenyl, 2-methyl-4-methoxyphenyl, 2-methyl-4-dimethylaminophenyl, 4-dimethylaminophenyl, phenoxy, methoxy, and dimethylamine. Electron-withdrawing groups on the framework included fluoro, cyano, and oxo substituents.

To determine whether these molecules can form a zwitterionic bond between **C1** and **C7**, we analyzed the energy gap between their diradical triplet and zwitterionic singlet states using the M06-2X^[38] density functional theory (DFT) method. The nature of the local minima was confirmed by evaluating the eigenvalues of the Hessian matrix. To ensure consistency, we examined selected molecules using additional DFT functionals, including ω -B97XD^[39], B3LYP^[40-42], and BLYP in a solvent environment. Although quantitative differences were expected, the selected molecules consistently exhibited a large singlet-triplet (S-T) gap, exceeding one-third of an eV, across all tested functionals. All calculations utilized the def2-TZVP basis set^[43,44] and were performed in both gas phase and solvent (dimethylformamide, DMF) using the SMD model.^[45] In the main text we solely focus on the results of M06-2X computations because this functional is known for relatively good performance in defining ground and excited-state energies and at the same time, its wavefunction can be used for full IQA analysis. DMF as a polar aprotic solvent notably stabilizes zwitterionic forms. Our initial analysis identified 36 local minimum structures with a low-energy singlet zwitterionic form in DMF, **Scheme S1**. However, in the gas phase, the number of molecules with a zwitterionic singlet ground state decreased to 24 due to destabilization of the zwitterionic singlet state. To further refine these results, we assessed the multireference character of the wavefunctions using the T1-diagnostic test at the coupled-

cluster computational level, **Table S3**.^[46] This test identified 23 molecules that passed the diagnostic criteria. Given the potential errors associated with DFT, we focused on molecules with an S-T energy gap exceeding 9 kcal.mol⁻¹ (roughly one-third of an electron-volt) to ensure robust predictions. This criterion excluded three additional molecules, leaving 20 systems for further analysis. Among these, six systems were substituted bicyclo[2.1.1]hexanes and bicyclo[1.1.1]pentanes. During optimization, some initial systems from these frameworks underwent ring-opening and alkyl-shift rearrangements. As a result, these four systems are excluded from the main text. All computations were performed utilizing the Gaussian 16 suite of programs.^[47] All QTAIM and IQA analyses were performed via AIMAll.^[48] NBO 3^[23] implemented in Gaussian was used for computation of NBO properties.

Acknowledgements

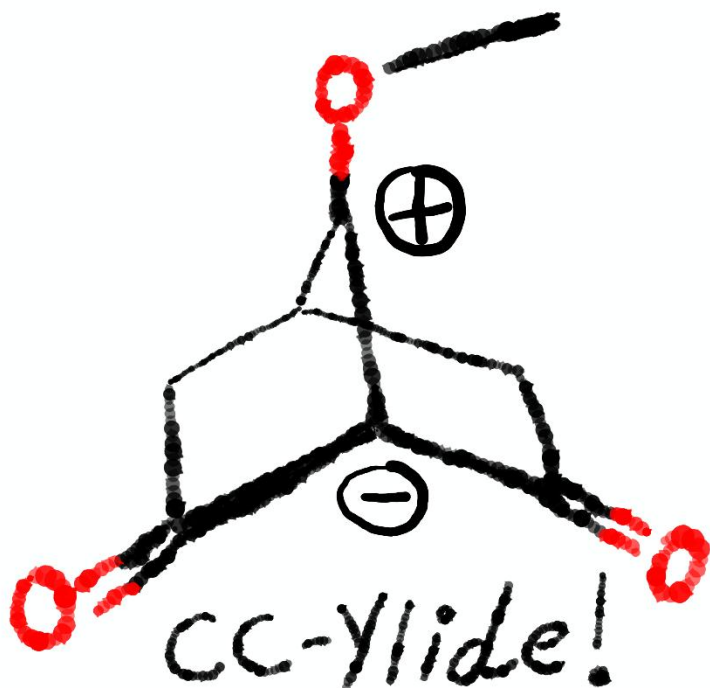
We would like to thank Przemysław Gaweł, Eli Zysman-Colman, and Oliver Dumele for their fruitful discussions about our proposed systems. We gratefully acknowledge Polish high-performance computing infrastructure PLGrid (HPC Centers: ACK Cyfronet AGH) for providing computer facilities and support within computational grant no. PLG/2024/017803. This work was financially supported by the Polish National Science Centre, Poland (OPUS 2020/39/B/ST4/02022).

References

- [1] T. Weng, Z. Xu, K. Li, Y. Guo, X. Chen, Z. Li, Z. Sun, *J. Am. Chem. Soc.* **2024**, *146*, 26454–26465.
- [2] J. Inoue, K. Fukui, T. Kubo, S. Nakazawa, K. Sato, D. Shiomi, Y. Morita, K. Yamamoto, T. Takui, K. Nakasuji, *J. Am. Chem. Soc.* **2001**, *123*, 12702–12703.
- [3] T. H. Dunning, W. J. Hunt, W. A. Goddard, *Chem. Phys. Lett.* **1969**, *4*, 147–150.
- [4] L. Salem, C. Rowland, *Angew. Chem. Int. Ed. Engl.* **1972**, *11*, 92–111.

- [5] H. M. Blatter, H. Lukaszewski, *Tetrahedron Lett.* **1968**, 9, 2701–2705.
- [6] H. K. Jr. Hall, A. B. Padias, *Acc. Chem. Res.* **1990**, 23, 3–9.
- [7] V. Lavallo, C. A. Dyker, B. Donnadieu, G. Bertrand, *Angew. Chem. Int. Ed.* **2009**, 48, 1540–1542.
- [8] L. Beverina, G. A. Pagani, *Acc. Chem. Res.* **2014**, 47, 319–329.
- [9] V. G. Machado, R. I. Stock, C. Reichardt, *Chem. Rev.* **2014**, 114, 10429–10475.
- [10] S. Arikawa, A. Shimizu, R. Shintani, *Angew. Chem. Int. Ed.* **2019**, 58, 6415–6419.
- [11] S. Mathieu, G. Trinquier, *Phys. Chem. Chem. Phys.* **2019**, 21, 5531–5565.
- [12] S. Mishra, D. Beyer, K. Eimre, S. Kezilebieke, R. Berger, O. Gröning, C. A. Pignedoli, K. Müllen, P. Liljeroth, P. Ruffieux, X. Feng, R. Fasel, *Nat. Nanotechnol.* **2020**, 15, 22–28.
- [13] D. Munz, K. Meyer, *Nat. Rev. Chem.* **2021**, 5, 422–439.
- [14] A. Shimizu, Y. Ishizaki, S. Horiuchi, T. Hirose, K. Matsuda, H. Sato, J. Yoshida, *J. Org. Chem.* **2021**, 86, 770–781.
- [15] F. Miao, Y. Ji, B. Han, S. M. Quintero, H. Chen, G. Xue, L. Cai, J. Casado, Y. Zheng, *Chem. Sci.* **2023**, 14, 2698–2705.
- [16] A. Hinz, J. Bresien, F. Breher, A. Schulz, *Chem. Rev.* **2023**, 123, 10468–10526.
- [17] C. Shu, Z. Yang, A. Rajca, *Chem. Rev.* **2023**, 123, 11954–12003.
- [18] J. Bredt, *Justus Liebigs Ann. Chem.* **1924**, 437, 1–13.
- [19] J. Y. W. Mak, R. H. Pouwer, C. M. Williams, *Angew. Chem. Int. Ed.* **2014**, 53, 13664–13688.
- [20] E. H. Krenske, C. M. Williams, *Angew. Chem. Int. Ed.* **2015**, 54, 10608–10612.
- [21] L. McDermott, Z. G. Walters, S. A. French, A. M. Clark, J. Ding, A. V. Kelleghan, K. N. Houk, N. K. Garg, *Science* **2024**, 386, eadq3519.
- [22] M. D. Summersgill, L. R. Gahan, S. Chow, G. K. Pierens, P. V. Bernhardt, E. H. Krenske, C. M. Williams, *Chem. Sci.* **2024**, 15, 19299–19306.
- [23] C. R. Landis, F. Weinhold, in *Chem. Bond*, John Wiley & Sons, Ltd, **2014**, pp. 91–120.
- [24] A. Martín-Pendás, M. A. Blanco, E. Francisco, *J. Chem. Phys.* **2004**, 120, 4581–4592.
- [25] M. A. Blanco, A. Martín Pendás, E. Francisco, *J. Chem. Theory Comput.* **2005**, 1, 1096–1109.
- [26] A. Martín-Pendás, E. Francisco, M. A. Blanco, *J. Comput. Chem.* **2005**, 26, 344–351.
- [27] E. Francisco, A. Martín-Pendás, M. A. Blanco, *J. Chem. Theory Comput.* **2006**, 2, 90–102.
- [28] R. F. W. Bader, *Atoms in Molecules: A Quantum Theory*, Clarendon Press, Oxford; New York, **1990**.
- [29] S. Sowlati-Hashjin, V. Šadek, S. Sadjadi, M. Karttunen, A. Martín-Pendás, C. Foroutan-Nejad, *Nat. Commun.* **2022**, 13, 2069.
- [30] M. Rafat, P. L. A. Popelier, in *Quantum Theory At. Mol. Solid State DNA Drug Des.* (Eds.: C.F. Matta, R.J. Boyd, A.D. Becke), Wiley-VCH, Weinheim, **2007**, pp. 121–139.
- [31] Z. Badri, C. Foroutan-Nejad, *Phys. Chem. Chem. Phys.* **2016**, 18, 11693–11699.
- [32] E. Francisco, D. Menéndez Crespo, A. Costales, Á. Martín-Pendás, *J. Comput. Chem.* **2017**, 38, 816–829.
- [33] S. Hirata, M. Head-Gordon, *Chem. Phys. Lett.* **1999**, 314, 291–299.
- [34] A. Endo, M. Ogasawara, A. Takahashi, D. Yokoyama, Y. Kato, C. Adachi, *Adv. Mater.* **2009**, 21, 4802–4806.
- [35] Z. Yang, Z. Mao, Z. Xie, Y. Zhang, S. Liu, J. Zhao, J. Xu, Z. Chi, M. P. Aldred, *Chem. Soc. Rev.* **2017**, 46, 915–1016.
- [36] X.-K. Chen, D. Kim, J.-L. Brédas, *Acc. Chem. Res.* **2018**, 51, 2215–2224.
- [37] T. Won, K. Nakayama, N. Aizawa, *Chem. Phys. Rev.* **2023**, 4, 021310.
- [38] Y. Zhao, D. G. Truhlar, *Theor. Chem. Acc.* **2008**, 120, 215–241.
- [39] J.-D. Chai, M. Head-Gordon, *Phys. Chem. Chem. Phys.* **2008**, 10, 6615–6620.
- [40] A. D. Becke, *Phys. Rev. A* **1988**, 38, 3098–3100.
- [41] A. D. Becke, *J. Chem. Phys.* **1993**, 98, 5648–5652.

- [42] C. Adamo, V. Barone, *J. Chem. Phys.* **1998**, *108*, 664–675.
- [43] F. Weigend, R. Ahlrichs, *Phys. Chem. Chem. Phys.* **2005**, *7*, 3297–3305.
- [44] F. Weigend, *Phys. Chem. Chem. Phys.* **2006**, *8*, 1057–1065.
- [45] A. V. Marenich, C. J. Cramer, D. G. Truhlar, *J. Phys. Chem. B* **2009**, *113*, 6378–6396.
- [46] T. J. Lee, P. R. Taylor, *Int. J. Quantum Chem.* **1989**, *36*, 199–207.
- [47] M. J. Frisch, G. W. Trucks, H. B. Schlegel, G. E. Scuseria, M. A. Robb, J. R. Cheeseman, G. Scalmani, V. Barone, G. A. Petersson, H. Nakatsuji, X. Li, M. Caricato, A. V. Marenich, J. Bloino, B. G. Janesko, R. Gomperts, B. Mennucci, H. P. Hratchian, J. V. Ortiz, A. F. Izmaylov, J. L. Sonnenberg, D. Williams-Young, F. Ding, F. Lipparini, F. Egidi, J. Goings, B. Peng, A. Petrone, T. Henderson, D. Ranasinghe, V. G. Zakrzewski, J. Gao, N. Rega, G. Zheng, W. Liang, M. Hada, M. Ehara, K. Toyota, R. Fukuda, J. Hasegawa, M. Ishida, T. Nakajima, Y. Honda, O. Kitao, H. Nakai, T. Vreven, K. Throssell, J. A. Montgomery, Jr., J. E. Peralta, F. Ogliaro, M. J. Bearpark, J. J. Heyd, E. N. Brothers, K. N. Kudin, V. N. Staroverov, T. A. Keith, R. Kobayashi, J. Normand, K. Raghavachari, A. P. Rendell, J. C. Burant, S. S. Iyengar, J. Tomasi, M. Cossi, J. M. Millam, M. Klene, C. Adamo, R. Cammi, J. W. Ochterski, R. L. Martin, K. Morokuma, O. Farkas, J. B. Foresman, D. J. Fox, **2016**.
- [48] T. A. Keith Gristmill Software, Overland Park KS, USA, 2019 (aim.tkgristmill.com), **2019**.



The norbornane-2,6-dione framework can accommodate a carbon-carbon ylide with a zwitterionic σ -bond.